Traffic Offloading via Markov Approximation in Heterogeneous Cellular Networks

Thant Zin Oo*, Nguyen H. Tran*, Walid Saad†*, Jaehyeok Son*, and Choong Seon Hong*,

*Department of Computer Science and Engineering, Kyung Hee University, Korea,
†Bradley Department of Electrical and Computer Engineering, Virginia Tech, USA,
Email: {tzoo, nguyenth, cshong}@khu.ac.kr, walids@vt.edu.

***Abstract*—The use of heterogeneous small cell-based networks to offload the traffic of existing cellular systems has recently attracted significant attention. One main challenge is solving the joint problems of user association, resource allocation, and interference mitigation. The goal of this paper is to design a self-organizing algorithm that can solve these problems, simultaneously. To this end, this joint resource allocation problem is formulated as an optimization problem which is then solved using log-sum-exp approximation. This solution is then shown to require complete information of the whole network which is not scalable with the network size. To address this scalability issue, a novel Markov chain approach is proposed and its transition probabilities are shown to eventually converge to the near optimal solution without complete information. Furthermore, the gap between the optimal and converged solutions is shown to be bounded. Simulation results show that our proposed algorithm effectively offloads the traffic from macro-cell base station to small-cell base stations. Moreover, the results also show that this algorithm converges very quickly independent of the number of possible configurations.**

***Index Terms*—Heterogeneous Cellular Networks, HetNets, Interference Mitigation, User Association, Resource Allocation.**

I. Introduction

The demand for wireless data traffic has increased considerably in the past decade and is expected to continue to grow in the next few years. However, mobile operator revenues are flattening due to saturated markets, flat-rate tariffs and competitive and regulatory pressure [1]. This decoupling of network traffic and operator revenue have led the mobile operators to increase the network efficiency in order to maximize their revenue. One viable solution is the deployment of multi-tier dense small-cell base stations (SBSs) overlaid on the existing macro cells. Economically, SBSs cost only a small fraction of the macro base stations (MBSs) in terms of both CAPEX and OPEX.

The major challenges for small cell based heterogeneous networks (HetNets) are user association (UA), resource allocation (RA) and interference mitigation (IM) [2]–[7]. Unlike classical wireless networks, in HetNets, the number of choices or configurations increases exponentially with the number of deployed SBSs. Thus, existing centralized resource management algorithms such as in [8] and [9] can no longer cope with the massive overhead in computation and signaling required by the HetNet small cells. This challenge is further exacerbated by the fact that UA, RA and IM are coupled and must be solved simultaneously. This problem becomes non-trivial when coordination and tradeoff are necessary between the competing interests of users and BSs. To address this problem, one must design self-organizing algorithms that can enable a small cell network to operate in a distributed manner and with little overhead [10]. Using self-organization, small cells can learn from their environment and autonomously adjust their configuration strategies towards achieving optimal performance. More importantly, self-organization mechanisms can be implemented distributedly without complete information and thus are scalable with network size [2].

A. Related Work

Game-theoretic approaches [2]–[4] are often used to analyze such self-organized mechanisms due to its unique ability to model the strategic interactions between competing interests of different players, i.e. BSs and users. Beyond game theory, the work in [5] studied joint RA and power control problem and proposed an optimal exhaustive algorithm and its corresponding sub-optimal distributed low-complexity algorithm. In [6], the authors focused on RA and inter-cell interference management and formulated the optimization problem into a low-complexity linear programming. In [7], considered success probability as a QoS constraint and formulated a throughput maximization problem to find the optimal spectrum allocation.

Recently, Markov approximation [11] was proposed to solve a number of combinatorial optimization problems such as in [11]–[13]. In [11], the authors presented three use cases, (i) utility maximization in CSMA networks, (ii) path selection in wire-line networks and (iii) channel assignment in wireless LANs. In [12], the authors applied Markov approximation to search for the optimal P2P network configuration distributedly for video streaming applications. Furthermore, Markov approximation was also employed in [13] for the joint virtual machine placement and routing in data-centers. However, these

This research was supported, in part, by Basic Science Research Program through National Research Foundation of Korea (NRF) funded by the Ministry of Education (NRF-2014R1A2A2A01005900), and in part, by the U.S. National Science Foundation under Grant CNS-1460316. Dr. C. S. Hong is the corresponding author.

978-1-5090-0223-8/16/$31.00 © 2016 IEEE

existing works do not take into account the fact that the UEs are only interested in maximizing their individual utilities whereas the BSs are concerned with minimizing their total costs which, in a distributed system, can lead to detrimental performance if not properly modeled.

B. Contributions

The main contribution of this paper is to address the joint problem of UA, IM and RA using Markov approximation. The main contributions of this paper are as follows:

- We formulate the joint problem of UA, RA and IM as an optimization problem whose goal is to maximize the downlink sum-rate of the network.
- We propose a Markov approximation framework to study the convergence in probability and the performance gap between optimal and approximate solutions.
- We then propose a distributed Markov Chain Directed Algorithm (MCDA) that is shown to converge in probability to a close-to-optimal solution.
- Simulation results verify that MCDA converges in probability.

The rest of the paper is organized as follows: In Section II, we present our system model. We formulate the problem in Section III. We present the Markov approximation in Section IV. We present our simulation results in Section V and we finally conclude this paper in Section VI.

II. System Model

Consider the downlink of a HetNet consisting of fixed BSs and randomly located UEs as illustrated in Fig. 1. The set of BSs is denoted by $\mathcal{B}$. Let $\mathcal{S}$ be the set of available sub-carriers that each BS $j \in \mathcal{B}$ can use. These sub-carriers will be further divided and allocated to the UEs associated to each BS j. We assume that each BS $j \in \mathcal{B}$ transmits with a constant per sub-carrier transmit power P_{jk} on sub-carrier k and total transmit power of BS j is $\hat{P}_j = \sum_{k\in\mathcal{S}} P_{jk}$. All BSs are connected to a high speed backhaul with negligible delay (such as a high speed fiber). Let $\mathcal{U}$ be the set of UEs located inside region $\mathcal{A}$ and $\psi_i \in \Psi$ be the requested downlink rate (bits per second) of UE i, where Ψ is the discrete set of QoS levels.

A. Data Rate and QoS

In this network, we consider a log-distance path loss model and the positive channel power gain between UE i and BS j can be calculated as: $h_{ij} = 10^{-\frac{\mu}{10}}$. We assume that each UE i is capable of measuring h_{ij} for all BSs $j \in \mathcal{B}$. Let $\mathcal{B}^{\mathcal{I}}_{jk} \subseteq \mathcal{B}$ be the set of BSs that interfere with BS j on sub-carrier k. Then, the instantaneous signal-to-interference-plus-noise-ratio (SINR) received at UE i from BS j on sub-carrier k is given as:

$$\Gamma_{ijk} = \frac{P_{jk}h_{ij}}{\sum_{m\in\mathcal{B}^{\mathcal{I}}_{jk}} P_{mk}h_{im} + WN_0}, \tag{1}$$

where W is the bandwidth of the sub-carrier and N_0 is the thermal noise spectral power. Note that the interference term is a function of the sub-carrier allocation, i.e., only those users who are allocated to the same sub-carriers will interfere with each other as detailed in Section II-B.

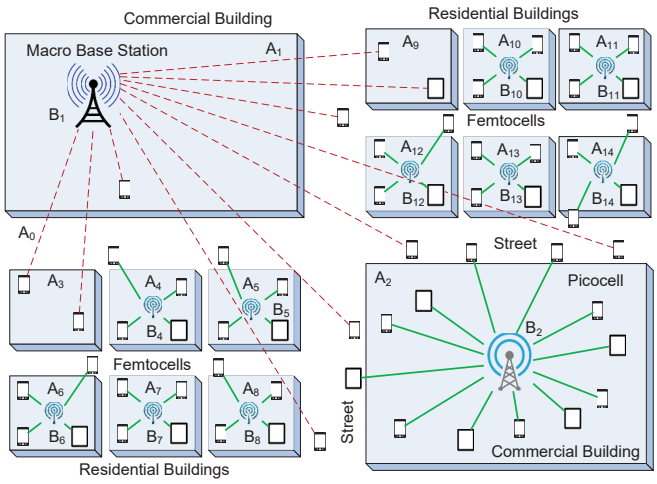

Fig. 1: An example of a three-tier HetNet including one macro-cell BS: $\{B_1\}$, one pico-cell BS: $\{B_2\}$, and ten femto-cell BSs: $\{B_4, \ldots, B_8, B_{10}, \ldots, B_{14}\}$. The pico-cell and femto-cell BSs are usually located at buildings that constitute hotspots for wireless traffic. Some buildings have no SBSs and the UEs located within these buildings will be served by the MBS. For example, buildings A_6 and A_9 are served by the MBS. Furthermore, UEs in an outdoor region, such as A_0, are either served by MBS or SBSs.

Accordingly, the achievable downlink rate from BS j to UE i on sub-carrier k is given by:

$$C_{ijk} = W \log_2(1 + \Gamma_{ijk}). \tag{2}$$

Then, the downlink rate of UE i will be given by:

$$R_i = \sum_{j\in\mathcal{B}} x_{ij}R_{ij} = \sum_{j\in\mathcal{B}}\sum_{k\in\mathcal{S}} x_{ij}y_{ik}C_{ijk}, \quad \forall i \in \mathcal{U}, \tag{3}$$

where $x_{ij} \in \{0, 1\}$ and $y_{ik} \in \{0, 1\}$ are the binary decision variables for user association and resource allocation, respectively.

A BS must serve its associated UEs with a minimum QoS requirement, i.e., $R_i \geq \psi_i$, $\forall i \in \mathcal{U}$. To do so, BS j must allocate minimum number of sub-carriers to UE i, which can be calculated as:

$$\textstyle\sum_{k\in\mathcal{S}} y_{ik} = \mathbb{1}^T \boldsymbol{y} = \left\lceil \dfrac{\psi_i}{C_{ijk}} \right\rceil, \tag{4}$$

where $\sum_{k\in\mathcal{S}} y_{ik}$ represents the total number of allocated sub-carriers, $\mathbb{1}$ is the vector of ones and $\lceil\cdot\rceil$ denotes the ceiling function.

B. Interference Mitigation and Spectrum Partitioning

Inter-tier IM is a key challenge in HetNets, since it can involve mutual interference between between a high-power BS (link) and a low-power BS (link). The high-power link usually blankets the low-power link with its interference, decreasing the low-power link's SINR. Thus, the low-power link might

need a large number of sub-carriers making it an expensive and unsustainable option. Hence, we isolate the high-power links from low-power links by using spectrum partitioning (SP) or orthogonal allocation [14].

We assume that the location of BSs are fixed and propose a dynamic SP scheme based on spectrum conflict graph and spectrum reuse graph. For BS j, another BS m is classified as belonging to either the conflict set $\mathcal{B}_j^{(\mathcal{C})}$ with high-interference links or the reuse set $\mathcal{B}_j^{(\mathcal{R})}$ with low-interference links, depending on the interference level from BS m to BS j. Thus, we have

$$\text{BS } m \in \begin{cases} \mathcal{B}_j^{(\mathcal{C})}, & \text{if } \min\{\Gamma_{ijk}, \Gamma_{imk}\} \leq \tilde{\Gamma}, \\ \mathcal{B}_j^{(\mathcal{R})}, & \text{otherwise,} \end{cases} \tag{5}$$

where $j \neq m,\ \forall j, m \in \mathcal{B},\ \mathcal{B}_{\mathcal{I}} = \{j\}$ and $\tilde{\Gamma} = 0\,\text{dB}$. Note that $\min\{\cdot\}$ is used since the interfering links are not symmetric due to disparity in transmission power.

The SP constraint for BS $j \in \mathcal{B}$ is given as:

$$\mathcal{S}_j \cap \mathcal{S}_m = \emptyset, \qquad \forall j \in \mathcal{B},\ \forall m \in \mathcal{B}_j^{(\mathcal{C})}, \tag{6}$$

$$\left|\bigcup_j \mathcal{S}_j\right| \leq |\mathcal{S}|, \qquad \forall j \in \mathcal{B}, \tag{7}$$

where $\mathcal{S}_j$ and $\mathcal{S}_m$ denote the sub-carriers assigned to BSs j and m, respectively.

Initially, the BSs will decide the partitions' boundaries by using (5) but not their sizes (i.e. number of sub-carriers in each partition). Depending on UE traffic demand, the partition sizes are changing dynamically with respect to the control variable y_{ik} which will be discussed further in next section. Let Υ denotes the incidence matrix (size: $|\mathcal{S}| \times |\mathcal{B}|$) which is shared by the BSs for sub-carrier allocation. This resembles to a graph multi-coloring problem [15] which jointly covers IM and RA, where $|\mathcal{S}|$-colors are assigned to $|\mathcal{B}|$ vertices. However, in this stage, our proposal only deals with IM with (5), (6) and (7).

III. Problem Formulation

Our goal is to design a mechanism that can offload as much traffic from MBS to SBSs as possible under given QoS constraints. Such an offload must be done in a self-organizing fashion.

A. Objective Function

We design the objective function as sum rate with pricing to optimize the social welfare of all UEs. The pricing captures the operating cost of BSs to reflect economic incentives. The objective function is given as:

$$U(\boldsymbol{x}, \boldsymbol{y}) = \sum_{i \in \mathcal{U}} \sum_{j \in \mathcal{B}} \sum_{k \in \mathcal{S}} x_{ij} y_{ik} (C_{ijk} - \lambda_j P_{jk}), \tag{8}$$

where C_{ijk} is given by (2). Here P_{jk} denotes the per sub-carrier transmit power of BS j, and λ_i denotes the unit transmit power price of BS j (whose unit of measurement is bits/s/Hz/W). Furthermore, the pricing term $-x_{ij}y_{ik}(\lambda_j P_{jk})$ reflects the tradeoff between UA, RA and IM. (8) incentivizes UEs to choose low power SBSs instead of MBS by pricing for higher powers. Finally, $\boldsymbol{x}$ (size $|\mathcal{U}| \times |\mathcal{B}|$) and $\boldsymbol{y}$ (size $|\mathcal{U}| \times |\mathcal{S}|$) are the control variables of the optimization problem. The elements x_{ij} and y_{ik} can only have binary values ('0' or '1').

B. Optimization Problem

We define the traffic offloading optimization problem under QoS provisioning as:

$$\underset{\boldsymbol{x},\boldsymbol{y}}{\text{maximize:}} \quad U(\boldsymbol{x}, \boldsymbol{y}), \tag{9}$$

$$\text{subject to:} \quad \sum_{j \in \mathcal{B}} x_{ij} \leq 1,\ \forall i \in \mathcal{U}, \tag{10}$$

$$\sum_{k \in \mathcal{S}} y_{ik} = \left\lceil \frac{\psi_i}{C_{ijk}} \right\rceil,\ \forall i \in \mathcal{U}, \tag{11}$$

$$\mathcal{S}_j \cap \mathcal{S}_m = \emptyset,\ \forall j \in \mathcal{B}, C\ \forall m \in \mathcal{B}_j^{(\mathcal{C})}, \tag{12}$$

$$\left|\bigcup_j \mathcal{S}_j\right| \leq |\mathcal{S}|,\ \forall j \in \mathcal{B}, \tag{13}$$

$$x_{ij} \in \{0, 1\},\ y_{ik} \in \{0, 1\}. \tag{14}$$

(10) is the association constraint which states that a UE can only be associated with at most one BS. (11) is the QoS constraint which is given in (4). (12) is interference constraint mentioned in (6) with dynamic spectrum partitioning scheme. (13), referred to as resource constraint, ensures that the sub-carriers allocated to UEs by BSs do not exceed total number of sub-carriers available to the network. Note that (10) is UE specific and BSs are responsible for (11), (12) and (13). Similarly, x_{ij} and y_{ik} correspond to the control decisions by UE i and BS j, respectively. This optimization problem is combinatorial and NP-hard.

C. Offloading Procedure

Our objective is to design a UE initiated self-organizing algorithm for data offload in HetNets. In the downlink, the UE is the receiver and, thus, it must take channel measurements for decision making. We let the UEs decide the association through the control variable x_{ij}. On the BS side, given the association, we minimize their OPEX through the control variable y_{ij}. Hence, the computationally expensive combinatorial aspect of UA is divided and distributed to all UEs, thus, simplifying the problem.

First, every UE i measures the received power from each BS j within its transmission range from its pilot signal. From the measured received signal strength, UE i calculates the minimum required sub-carriers for its traffic demand that satisfies the QoS constraint (11).

Then, UE i sends its request to the BS j that it has chosen to associate with. The action of each UE i, $\boldsymbol{x}_i$ is a vector (size $|\mathcal{B}| \times 1$). As presented in Fig. 2a, when a given UE i sends request to BS j, its corresponding element, $x_{ij} = 1$. The request contains the required data rate, the number of sub-carriers needed to satisfy its QoS constraint (11) and the time duration of the request. Note that UE i can only send one request at any one time according to the association constraint (10).

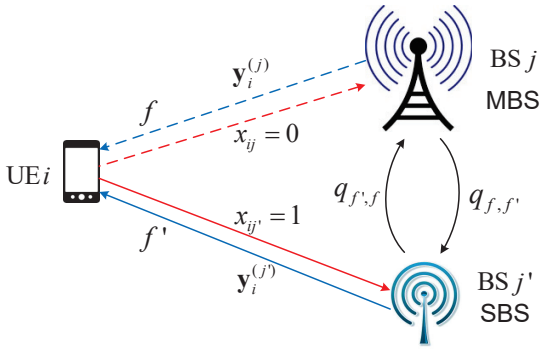

x_{ij} request from UE i to BS j
$x_{ij'}$ request from UE i to BS j'
$\mathbf{y}_i^{(j)}$ subcarriers allocated to UE i by BS j
$\mathbf{y}_i^{(j')}$ subcarriers allocated to UE i by BS j'

(a) Change in network configuration.

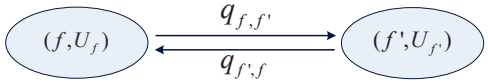

(b) Corresponding Markov chain.

Fig. 2: Transition rates from configuration f to f'

Subsequently, BS j will either accepts or rejects the traffic request from the UE i depending on its available resources, i.e. (12) and (13). The acceptance of a request is indicated by the allocation of sub-carriers in the form of a reply with sub-carriers frequencies to UE i, i.e. $\boldsymbol{y}_i$ (size $|\mathcal{S}| \times 1$) as depicted in 2a. The BS j will simply not reply in case of a rejection, i.e. $\boldsymbol{y}_i$ be a vector of zeros.

Finally, BS j will update Υ which is used to monitor the availability of resources and to ensure the resource constraint (13) is not violated. The updated Υ matrix is then broadcast to other BS via the back haul.

IV. Traffic Offloading via Markov Approximation

The optimization problem (**SRM-P**) is combinatorial and NP-hard without any computationally efficient solution. Thus, we adopt Markov approximation [11], [12] to solve (**SRM-P**) because of its ability to solve multiple sub-problems simultaneously without disjoint step-by-step solutions. Markov approximation framework consists of two steps: log-sum-exp approximation and constructing problem-specific Markov chains that allow distributed implementation.

Let $f = \{\boldsymbol{x}, \boldsymbol{y}\}$ be a configuration of the network, Ω denotes the set of all possible configurations, and $\mathcal{F} \subset \Omega$ denotes the set of all the feasible configurations of the network defined by (10)–(13). For ease of presentation, we let $U_f = U(\boldsymbol{x}, \boldsymbol{y})$. Thus, we have

$$\max_{f \in \mathcal{F}} \quad U_f \tag{15}$$

and its equivalent maximum weight independent set (MWIS) problem is:

$$\begin{aligned} \max_{\boldsymbol{p} \geq 0} \quad & \textstyle\sum_{f \in \mathcal{F}} p_f U_f \\ \text{s.t.} \quad & \textstyle\sum_{f \in \mathcal{F}} p_f = 1. \end{aligned} \tag{16}$$

where p_f is the probability of choosing configuration f, i.e. its weight. (16) is still hard to solve since the number of variables is still combinatorial.

A. Log-sum-exp Approximation

Following the framework, we apply log-sum-exponential approximation [11] [16, p. 72] to (15) as,

$$\max_{f \in \mathcal{F}} U_f \approx \tfrac{1}{\beta} \log \left[\textstyle\sum_{f \in \mathcal{F}} \exp(\beta U_f) \right], \tag{17}$$

where β is a positive constant. Let $|\mathcal{F}|$ be the size of set $\mathcal{F}$, then the approximation accuracy is given as [11] [16, p. 72]:

$$\max_{f \in \mathcal{F}} U_f \leq \frac{1}{\beta} \log \left[\sum_{f \in \mathcal{F}} \exp(\beta U_f) \right] \leq \max_{f \in \mathcal{F}} U_f + \frac{1}{\beta} \log |\mathcal{F}|. \tag{18}$$

As $\beta \to \infty$, $\frac{1}{\beta} \log |\mathcal{F}| \to 0$, and the approximation becomes exact.

The log-sum-exp approximation in (17) is equivalent to solving the following optimization problem [11] [16, p. 93],

$$\begin{aligned} \max_{\boldsymbol{p} \geq 0} \quad & \underbrace{\textstyle\sum_{f \in \mathcal{F}} p_f U_f}_{\text{MWIS objective}} - \underbrace{\tfrac{1}{\beta} \textstyle\sum_{f \in \mathcal{F}} p_f \log p_f}_{\text{entropy term}} \\ \text{s.t.} \quad & \textstyle\sum_{f \in \mathcal{F}} p_f = 1. \end{aligned} \tag{19}$$

By solving the Karush-Khun-Tucker (KKT) conditions [16, p. 243] of the optimization problem given in (19), we obtain the optimal probability distribution, $\boldsymbol{p}^*$, which is given by

$$p_f^*(U_f) = \frac{\exp(\beta U_f)}{\sum_{f' \in \mathcal{F}} \exp(\beta U_{f'})}, \quad \forall f \in \mathcal{F}. \tag{20}$$

The optimal solution in (20) is an implicit solution for equivalent MWIS problem given in (16), off by an *entropy* term $-\frac{1}{\beta} \sum_{f \in \mathcal{F}} p_f \log p_f$. (18) provides the approximation gap (19). However, (19) requires *completeness*, i.e. complete information on $\mathcal{F}$ which is typically unknown due to the large computational space. Thus, to obtain $\mathcal{F}$, we must solve the feasibility problem on Ω which is computationally exhaustive.

B. Markov Chain and Transition Rate

The next step in the framework is to design a problem specific MC. Each state f represents a configuration with its corresponding stationary distribution $p_f^*(U_f)$ given in (20) and the set of states $\mathcal{F}$ represents all possible configurations. As the MC converges, the configurations will be time-shared according to p_f^*. Hence, the network will operate in the best configurations most of the time. It was proven in [11] that for any probability distribution of the product form $p_f^*(U_f)$ given in (20), there exists at least one continuous-time time-reversible ergodic MC whose stationary distribution is $p_f^*(U_f)$.

Let configurations $f, f' \in \mathcal{F}$ be the states of a time-reversible ergodic MC with stationary distributions $p_f^*(U_f)$, $(f \in \mathcal{F})$ in (20). Let $q_{(f \to f')}$ and $q_{(f' \to f)}$ denote the non-negative transition rates from $f \to f'$ and $f' \to f$, respectively. Then the two following conditions are sufficient to allow a large degree of freedom in algorithm design [11]:

- Any two states are reachable from each other,

- The balanced equation, (21), is satisfied for all $f, f' \in \mathcal{F}$,

$$\begin{aligned} p_f^*(U_f)\; q_{(f\to f')} &= p_{f'}^*(U_{f'})\; q_{(f'\to f)}, \\ \exp(\beta U_f)\; q_{(f\to f')} &= \exp(\beta U_{f'})\; q_{(f'\to f)}. \end{aligned} \tag{21}$$

The balance equation in (21) is significant because complete information on all possible configurations, $\mathcal{F}$, is no longer necessary. Moreover, as long as (21) is satisfied, any $q_{(f\to f')}$ and $q_{(f'\to f)}$ values can be used to design an algorithm.

We consider the difference in utilities $(U_{f'} - U_f)$ as in [11] and keep the *symmetry* as in [12]. Thus, we have

$$q_{(f\to f')} = \exp(-\tau)\cdot\left(1+\exp[\beta\,(U_f - U_{f'})]\right)^{-1} \tag{22}$$

$$q_{(f'\to f)} = \exp(-\tau)\cdot\left(1+\exp[\beta\,(U_{f'} - U_f)]\right)^{-1} \tag{23}$$

where τ is a positive constant. (22)–(23) are logistic functions of utility differences and have closed-form expressions in terms of p_f^* and $p_{f'}^*$ given in (24)–(25).

$$q_{(f\to f')} = \exp(-\tau)\cdot p_{f'}^*\cdot\left(p_f^* + p_{f'}^*\right)^{-1}, \tag{24}$$

$$q_{(f'\to f)} = \exp(-\tau)\cdot p_f^*\cdot\left(p_f^* + p_{f'}^*\right)^{-1}. \tag{25}$$

The earlier discussion on the approximation gap still holds. For instance, consider following three different scenarios,

- $\beta\to\infty$ and $U_f > U_{f'} \Rightarrow \exp[\beta(U_{f'} - U_f)] \to 0$.
  - Hence, UE i will choose BS j with $q_{(f'\to f)} \approx 1$.
- $\beta\to\infty$ and $U_f < U_{f'} \Rightarrow \exp[\beta(U_f - U_{f'})] \to 0$.
  - Thus, UE i will choose BS j' with $q_{(f'\to f)} \approx 1$.
- $\beta = 0$ or $U_f = U_{f'} \Rightarrow q_{(f\to f')} = q_{(f'\to f)} = \frac{1}{2}$.
  - Thus, UE i choose BS j or j' with equal probability.

C. Markov Chain Directed Algorithm

The next challenge is to convert the designed transition rates into an effective algorithm. Note that all transition rates presented in Section. IV-B is a function of U_f, the social utility of the whole network. However, due to the distributed nature of the network itself, an UE can only know its own utility without additional signaling. This poses a huge challenge in computing $q_{(f\to f')}$ and $q_{(f'\to f)}$.

Hence, we initially assumed *singularity*, i.e. only one UE is allowed to change its configuration at one time epoch as depicted in Fig. 2, i.e. $\{\boldsymbol{x},\boldsymbol{y}\} \to \{\boldsymbol{x}',\boldsymbol{y}'\} \equiv \{\boldsymbol{x}_i,\boldsymbol{y}_i\} \to \{\boldsymbol{x}_i',\boldsymbol{y}_i'\}$. In other words, the change in f is limited to a single element. Let $f_i = \{\boldsymbol{x}_i,\boldsymbol{y}_i\}$, then $(U_{f'} - U_f) = (U_{f_i'} - U_{f_i}) = (R_{ij'} - R_{ij})$. Thus, we substitute individual utilities in (22)–(23) and set $\tau = 0$ to calculate $q_{(f\to f')}$ and $q_{(f'\to f)}$:

$$q_{(f\to f')} = \exp(-\tau)\cdot\left(1+\exp[\beta\,(R_{ij} - R_{ij'})]\right)^{-1} \tag{26}$$

$$q_{(f'\to f)} = \exp(-\tau)\cdot\left(1+\exp[\beta\,(R_{ij'} - R_{ij})]\right)^{-1} \tag{27}$$

In practice, we relax the *singularity* assumption since more than one UE can change their configurations at any given time. In this case, without additional signaling, measurements taken by UE i becomes out-of-date when another UE i' changes its configuration, i.e. $(U_{f'} - U_f) \neq (R_{ij'} - R_{ij})$. However, for a distributed algorithm, the signaling overhead will increase rapidly with number of UEs and BSs. Therefore, we keep using (26)–(27) with individual utilities as the transition rates for our proposed Markov chain directed distributed algorithm (MCDA) described in Algorithm 1, i.e. the *completeness* assumption is relaxed. MCDA solves (**SRM-P**) in a repeated manner and has two distinct phases *exploration* and *exploitation*. In *exploration* phase, UE i experiments by finding a random feasible configuration to implement. In *exploitation* phase, UE i compares the current utility obtained from experimentation with previously achieved utility. UE i probabilistically choose the configuration which achieves maximum utility. This *exploration–exploitation* steps are repeated until an equilibrium is reached, i.e. the underlying MC converges to the stationary distribution. After a sufficiently large number of time epochs, MCDA converges in probability to a close to optimal solution. The gap between optimal distribution $p_f^*(U_f)$ and the converged distribution will further be discussed in Section IV-D.

Algorithm 1: Markov chain guided distributed algorithm

Let $\mathcal{U}_p \subseteq \mathcal{U}$ be set of participating UEs and $\tau = 0$.
Initialization: $\mathcal{U}_p := \mathcal{U}$ *and each UE* $i \in \mathcal{U}$
- Measure pilot signals from $\forall j \in \mathcal{B}$.
- Calculate required sub-carriers using (4).
- Send request to MBS which serves requests in a FIFO fashion.
- Calculate its utility $U_{f_i} = R_{ij}$ using (3).

for $t \in \{1, 2, \cdots, T\}$, *and* $\forall i \in \mathcal{U}_p$ **do**
- **Exploration:** *If UE* i *did not explore in iteration* t,
  - UE i chooses a feasible BS $j' \neq j,\ j', j \in \mathcal{B}$.
  - UE i sends request to BS j' as in Fig. 2.
  - **if** *BS* j' *has enough resources* **then**
    - BS j' find sub-channels using (6).
    - BS j' will reply with sub-channels, $\boldsymbol{y}_i^{(j')}$.
  - **else**
    - BS j' will not reply, i.e. $\boldsymbol{y}_i^{(j')} = [0, 0, \cdots, 0]$.
  - UE i calculates its utility $R_{ij'}$ using (3).
- **Exploitation:** *If UE* i *explored in iteration* t,
  - UE i calculates $q_{(f\to f')}$ using (26).
  - *UE* i *will choose either BS* j' *or* j *as follows:*
    - Stay with BS j' with prob. $q_{(f\to f')}$.
    - Revert back to BS j, with prob. $1 - q_{(f\to f')}$.
- BS j updates resource usage matrix, Υ.
- BS j broadcasts Υ to all BSs.

D. Gap between Optimal and Converged Distributions

Since we use individual transition rates as given by (26)–(27), the output of MCDA may not converge to the desired stationary distribution $p_f^*(U_f)$. For each configuration $f \in \mathcal{F}$, let $[-\delta_f, \delta_f]$ be the bounded inaccuracy region for exact utility U_f . δ_f can be different for different f. For ease of presentation, we assume that the inaccurate utilities for configuration f only takes one of the following $2n_f+1$ discrete values: $[U_f - \delta_f, \cdots, U_f - \frac{1}{n_f},\ U_f,\ U_f + \frac{1}{n_f}\delta_f, \cdots, U_f + \delta_f]$, where n_f is a positive constant. Moreover, with probability $\eta_{j,f}$, the inaccurate utility takes the value $U_f + \frac{j}{n_f}\delta_f,\ \forall j \in \{-n_f, \cdots, n_f\}$ and $\sum_{j=-n_f}^{n_f}\eta_{j,f} = 1$.

To capture and study the inaccuracies of real-life transitions, we construct an extended MC. In the extended MC, a state is associated with a configuration and an inaccurate utility. For

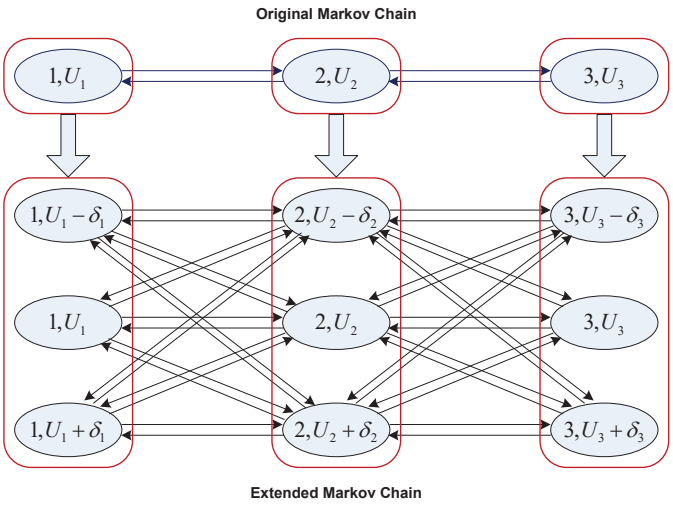

Fig. 3: An example 3-state original MC and its corresponding extended MC. For each configuration $f \in \{1,2,3\}$, the inaccurate utilities take values $\{U_f-\delta_f,\ U_f,\ U_f+\delta_f\}$ with probability $\{\eta_{-1,f},\ \eta_{0,f},\ \eta_{1,f}\}$, respectively.

any configuration $f \in \mathcal{F}$ and its corresponding U_f, there are $2n_f+1$ states in the extended MC: $\left(f, U_f+\frac{j}{n_f}\delta_f\right),\ j \in \{-n_f,\cdots,n_f\}$. Furthermore, as direct transitions exist between configurations f and f' in the original MC, direct transitions must also exist between states $\left(f, U_f+\frac{j}{n_f}\delta_f\right)$ and $\left(f', U_{f'}+\frac{j'}{n_{f'}}\delta_{f'}\right),\ \forall j \in \{-n_f,\cdots,n_f\},\ j' \in \{-n_{f'},\cdots,n_{f'}\}$ in the corresponding extended MC. An example extended MC is depicted in Fig. 3. For notational convenience, we let $U_0 = U_f+\frac{j}{n_f}\delta_f$, $U_0' = U_{f'}+\frac{j'}{n_{f'}}\delta_{f'}$, and $(s_j \to s_j') = (f, U_0) \to (f', U_0')$.

Based on the transition rates for the orignial MC in (22) and (23), the transition rates for the extended MC are designed as:

$$q_{(s_j \to s_j')} = \eta_{j,f}\exp(-\tau)\cdot\left(1+\exp[\beta(U_0-U_{0'})]\right)^{-1}, \quad (28)$$

$$q_{(s_j' \to s_j)} = \eta_{j,f}\exp(-\tau)\cdot\left(1+\exp[\beta(U_{0'}-U_0)]\right)^{-1}, \quad (29)$$

where $\sum_{j=-n_f}^{n_f}\eta_{j,f} = 1$ and $\sum_{j'=-n_f}^{n_f}\eta_{j',f'} = 1$. The extended MC is *irreducible* and only has a *finite* number of states under the assumption of discrete bounded inaccurate utilities. Thus, its stationary distribution is *unique*.

Let $\tilde{\boldsymbol{p}}$ and $\bar{\boldsymbol{p}}$ be the stationary distributions of the *states* and *configurations* in the extended MC, respectively. Then,

$$\tilde{\boldsymbol{p}} \triangleq [\tilde{p}_{(f,U_f+\frac{j}{n_f}\delta_f)},\ j \in \{-n_f,\cdots,n_f\},\ f \in \mathcal{F}], \quad (30)$$

$$\bar{\boldsymbol{p}} \triangleq [\bar{p}_f(\boldsymbol{U}),\ f \in \mathcal{F}], \quad (31)$$

$$\bar{p}_f(\boldsymbol{U}) = \textstyle\sum_{j\in\{-n_f,\cdots,n_f\}}\tilde{p}_{(f,U_f+\frac{j}{n_f}\delta_f)},\ \forall f \in \mathcal{F}, \quad (32)$$

since for any $f \in \mathcal{F}$, there are $2n_f+1$ states associated with f in the extended MC.

We apply the total variation distance [12], [17] to quantify the difference between $\boldsymbol{p}^*$ and $\bar{\boldsymbol{p}}$ as:

$$d_{TV}(\boldsymbol{p}^*, \tilde{\boldsymbol{p}}) \triangleq \tfrac{1}{2}\textstyle\sum_{f\in\mathcal{F}}\left|p_f^* - \tilde{p}_f\right|. \quad (33)$$

[12] have proved that $d_{TV}(\boldsymbol{p}^*, \tilde{\boldsymbol{p}})$ are bounded as follows:

$$0 \le d_{TV}(\boldsymbol{p}^*, \tilde{\boldsymbol{p}}) \le 1-\exp(-2\beta\delta_{\max}), \quad (34)$$

where $\delta_{\max} = \max_{f\in\mathcal{F}}\delta_f$, and $U_{\max} = \max_{f\in\mathcal{F}}U_f$. Moreover, the optimal gap between the utilities is bounded as follows:

$$0 \le \left|\boldsymbol{p}^*\boldsymbol{U}^T - \tilde{\boldsymbol{p}}\boldsymbol{U}^T\right| \le 2U_{\max}(1-\exp(-2\beta\delta_{\max})). \quad (35)$$

The use of the Markov approximation framework enables us to solve combinatorial problems with very large configuration space without any information on the configurations themselves. We only need to design a Markov chain and its transition rates that will converge to the stationary distribution. Furthermore, the upper bounds on $d_{TV}(\boldsymbol{p}^*, \tilde{\boldsymbol{p}})$ given in (34) and the optimal gap given in (35) do not depend on the number of configurations $|\mathcal{F}|$, the values of n_f, and the distributions of inaccurate utilities, $\eta_{j,f},\ (-n_f \le j \le n_f,\ f \in \mathcal{F})$. Specifically, in HetNets, each UE needs to know just its own utility removing the costly overhead of signaling to learn other UEs utilities and enabling a completely distributed algorithm. The significance is that the problem formulation is designed as a social welfare utility in (**SRM-P**) and we can achieve a bounded sub-optimal solution with a distributed self-organized algorithm. Additionally, the upper bounds in (34) and (35) decrease exponentially as the worst inaccuracy bound $\delta_{\max}$ decreases. For our case, the isolation of large interfering links by (6) makes the value of $\delta_{\max}$ small. Thus, (26)–(27) remains valid. Moreover, a *irreducible* and *finite* Markov chain (i.e. the extended Markov chain) will converge with probability one and its *mixing-time* characterizes its converge rate [18]. Hence, MCDA will converge to a close-to-optimal solution.

V. Simulation Results and Analysis

We perform extensive simulations to evaluate our proposed algorithms. The main simulation parameters are given in Table I.

First, for all our experiments, we assume the BSs to be deployed at fixed locations. Second, we randomly deploy UEs following a homogeneous PPP for different experiments. Third, we consider discrete user demands (i.e. requested data rate) whose probability mass function (PMF) is a binomial distribution. In this network, we consider a log-distance path loss model, as given by:

$$\mu = \mu_0 + 10\,\zeta\log_{10}\frac{d}{d_0} + X_g, \quad (36)$$

where μ is the total path loss in (dB), μ_0 is the path loss at reference distance d_0 for the BS, d is the length of transmission path, ζ is the path loss exponent, and X_g is the attenuation in dB caused by fading. Moreover, we assume that

- for indoors, $d \le 20$ m, $\zeta = 3$, and X_g is a Gaussian random variable with zero mean and standard deviation σ reflecting attenuation caused by shadow fading.

TABLE I: Default Simulation Parameters

Quantity	Values
Area of region (A)	$200\text{ m} \times 200\text{ m}$
UE population ($\lvert\mathcal{U}\rvert$)	100
UE traffic demand (ψ_i)	$[0.1, 1]$ Mbps
# of BS ($\lvert\mathcal{B}\rvert = \lvert\mathcal{B}_\text{m} \cup \mathcal{B}_\text{p} \cup \mathcal{B}_\text{f}\rvert$)	$20 = 1 + 2 + 17$
Total transmit power of BSs	$\{46, 36, 26\}$ dBm
Antenna gain of BSs (G)	$\{12, 6, 3\}$ dBi
Reference distance of BSs (d_0)	$\{1000, 100, 20\}$ m
Transmit antenna height of BSs (h_t)	$\{30, 10, 3\}$ m
# of sub-carriers ($\lvert\mathcal{S}\rvert$)	12×100
Bandwidth of each sub-carrier (W)	15 kHz
Thermal noise for 1 Hz at 20 ° C	-174 dBm
Gaussian parameters of X_g	$\text{E}[X_g] = 0,\ \sigma = 0.5$
Rayleigh parameter of X_g	$\sigma = 0.5$
Unit price of transmit power (λ)	1000
Parameter β	700

- for outdoors, $d > 20$ m, $\zeta = 4$, and X_g is a Rayleigh random variable for fast fading;

The reference path loss is calculated using two-ray ground reflection model as

$$\mu_0 = 40\log_{10}(d_0) - 10\log_{10}(Gh_t^2h_r^2), \tag{37}$$

where G is the transmit antenna gain, h_t and h_r are the heights of the antenna of transmitter and receiver, respectively.

A. Convergence

We performed experiments to test the convergence of MCDA. For this experiment, we randomly deployed $|\mathcal{U}| = 100$ UEs and run the simulations for 2000 iterations. For notational convenience, we attach the prefix 'Avg-' to represent average value and the suffixes '-s' and '-p' to describe the *singular* and *parallel* operations, respectively. In *singular* operation, the singularity assumption holds and only one UE can change its configuration in one time slot whereas in *parallel* operation, all UEs can change their configurations in one time slot.

Fig. 4 shows the convergence of the MCDA approach. Periodic fluctuations can be seen for the instantaneous values of singular and parallel operations in Fig. 4. In contrast, the average values of singular and parallel operations gradually converges as depicted in Fig. 4 due to convergence in probability to the stationary distribution of the Markov chain. Note that average values of singular and parallel operations corresponds to $\boldsymbol{p}^*\boldsymbol{U}^T$ and $\tilde{\boldsymbol{p}}\boldsymbol{U}^T$, respectively. As shown in Fig. 4b, the average total cost of singular operation converges slowly because of its dependence on the number of UEs. For this experiment, convergence starts at around 1970 iterations to 0.02 unit deviation in total cost. On the other hand, the average total cost of parallel operation does not depend on the number of UEs and takes less then 250 iterations (approximately 8 times faster) to converge to a 0.02 unit deviation. The gap between the average sum-rates of single and parallel operations is governed by the bound given in (35).

In Fig. 4a, we can see that the average sum-rate of parallel operation sharply increases and then begins to decrease. The sharp increase is due to the initial *exploration* for feasible configurations of all UEs, which were associated to MBS at first. After each successive *exploration*, the UEs will perform

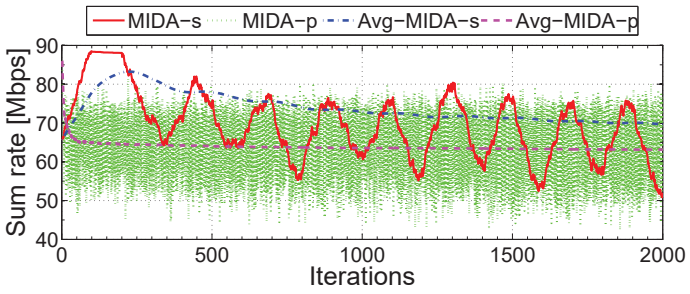

(a) Sum rate versus iterations.

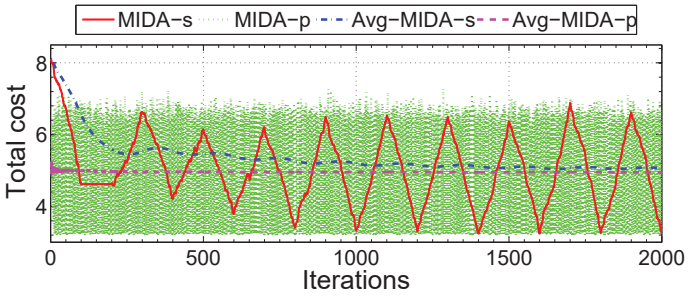

(b) Total cost versus iterations.

Fig. 4: Convergence of MCDA, $|\mathcal{U}| = 100$.

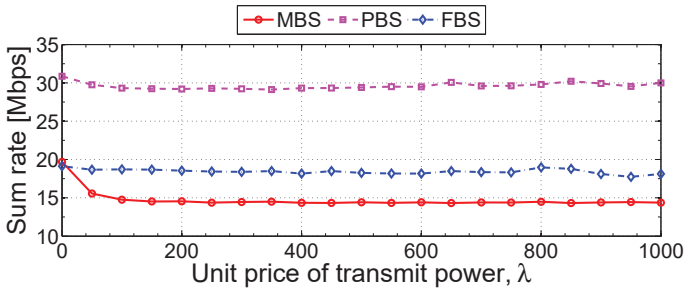

Fig. 5: Effect of λ on MCDA, $|\mathcal{U}| = 100$.

exploitation, i.e. probabilistically choose the configuration with maximum profit. Hence, some high data rate configurations are abandoned due to their high cost. The corresponding initial *exploration* cost is depicted in Fig. 4b. In contrast, average sum-rate of singular operation rises and drops back slowly since only a UE changes its configuration in a time slot as depicted in Fig. 4. Note that it will eventually converges to the optimal distribution $\boldsymbol{p}^*$.

B. Effect of Key Parameters

1) Effect of unit price of transmit power λ: The unit price of transmit power (λ) is given in (8). λ can decides how much traffic is offloaded from MBS to SBSs. We performed an experiment to study the effects on λ on MCDA for $|\mathcal{U}| = 100$. The average sum-rate is broken down into respective BS-tiers as shown in Fig. 5. The MBS has the highest transmission power ($\hat{P}_j$), followed by PBSs in second place and FBSs have the lowest power. MCDA is maximizing the sum rate while minimizing the cost at the same time as defined in (8). λ represents the weight that decides whether maximization or

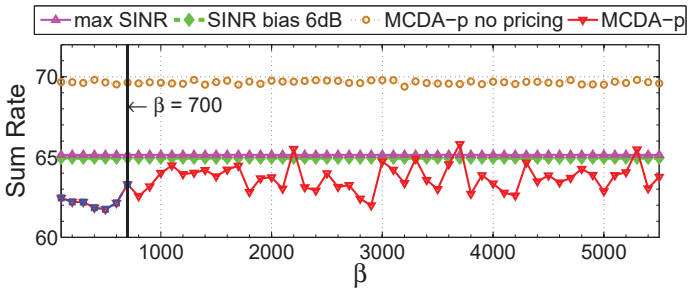

(a) The effects of β on the sum rate.

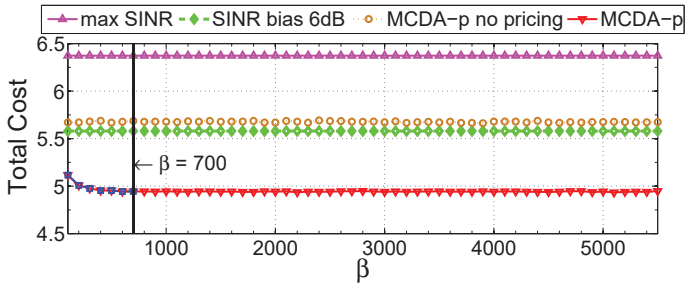

(b) The effects of β on the total cost.

Fig. 6: Comparison with other schemes, $|\mathcal{U}| = 100$, $\lambda = 1000$. [12] uses log-linear function of utilities which is bounded at $\beta = 700$. The logistic function of difference in utilities (22)–(23) increases the bound to $\beta = 5500$.

minimization is prioritized. Hence, the algorithms offload the traffic from high power MBS to low power PBSs and FBSs. As shown in Fig. 5, PBS-tier has the highest sum rate, followed by FBS-tier in second place and MBS-tier has the lowest sum rate. Moreover, the sum rate of MBS-tier decreases with the increasing λ. This is more evident during $0 \leq \lambda < 200$, where sum rates of MBS-tier and PBS-tier drops exponentially. During $200 \leq \lambda < 600$, there is not much variations in the sum rates of all BS tiers. During $600 \leq \lambda < 1000$, sum rate of MBS-tier remains almost constant whereas, those of PBS-tier and FBS-tier increases gradually with minor fluctuations. At $\lambda = 1000$, sum rates of MBS, PBS and FBS tiers are approximately $\{14.5, 30, 18\}$ Mbps, respectively.

2) Effect of parameter β: As discussed in Section IV-A, the parameter β has a significant impact on Markov approximation. For the MCDA to approach the optimal solution, in theory, $\beta \to \infty$. In practice, that is not possible and we explore the effect of β by conducting an experiment. As shown in Fig. 6b, as the value of β increases, the total cost decreases for MCDA. This agrees with earlier discussions in Section IV-A. However, there exists an upper limit in which we can calculate the exponential $\exp(c)$ (e.g. in Matlab $c = 709$). Thus, we must design transition rates that can use the maximum β bounded by the computation constraint. For example, [12] designs $q_{(f \to f')}$ and $q_{(f' \to f)}$ as log-linear function of utilities. Thus, $q_{(f \to f')}$ and $q_{(f' \to f)}$ design in [12] can only choose $\beta = 700$ at most. On the other hand, our design given in (22)–(23) uses logistic function of utility difference and can choose up to $\beta = 5500$. In [12], $\exp(\beta\, U_f)$ and $\exp(\beta\, U_{f'})$ is computed which limits the value of β. In contrast, (22) computes only $\exp[\beta\, (U_{f'} - U_f)]$ which allows β to have a larger value.

Furthermore, the comparison with other schemes are shown in Fig. 6. As shown in Fig. 6b, MCDA has the lowest operating cost. In Fig. 6a, MCDA without pricing (i.e. $\lambda = 0$) performs the best since it disregards the operating costs incurred by the BSs. By taking into account the BS operating cost (i.e. $\lambda > 0$), MCDA allocates just the minimum number of sub-carriers required to UEs, and thus, have the lowest sum-rate in Fig. 6a.

VI. Conclusions

In this paper, we have analyzed the traffic offloading from macro-cell base stations to small-cell base stations using a Markov approximation framework. We have formulated three joint sub-problems of user association, resource allocation and interference mitigation as the maximization of sum-rate with pricing. We have designed a problem specific Markov chain and have introduced appropriate transition probabilities that ensure convergence, in probability, to a close-to-optimal solution. After relaxing the assumptions made in Markov approximation framework, we have designed a Markov chain guided algorithm (MCDA) using which the network can self-organize to offload traffic from MBS to SBSs. The designed MCDA is shown to converge to a bounded close-to-optimal solution. Simulation results verify the convergence of MCDA and the traffic offload from MBS to SBSs. Furthermore, our proposed approach is also shown to further decrease the total operating costs of the network.

References

[1] B. Molleryd, J. Markendahl, J. Werding, and O. Makitalo, "Decoupling of revenues and traffic - is there a revenue gap for mobile broadband?" in *9th Conference on Telecommunications Internet and Media Techno Economics*, Ghent, Belgium, June 2010.

[2] M. Bennis, S. Perlaza, P. Blasco, Z. Han, and H. Poor, "Self-organization in small cell networks: A reinforcement learning approach," *IEEE Trans. on Wireless Communications*, vol. 12, no. 7, pp. 3202–3212, July 2013.

[3] J. Marden and J. Shamma, "Revisiting log-linear learning: Asynchrony, completeness and payoff-based implementation," in *48th Annual Allerton Conference on Communication, Control, and Computing*, Monticello, Illinois, September 2010, pp. 1171–1172.

[4] D. Niyato and E. Hossain, "Dynamics of network selection in heterogeneous wireless networks: An evolutionary game approach," *IEEE Trans. on Vehicular Technology*, vol. 58, no. 4, pp. 2008–2017, May 2009.

[5] V. N. Ha and L. B. Le, "Fair resource allocation for OFDMA femtocell networks with macrocell protection," *IEEE Trans. on Vehicular Technology*, vol. 63, no. 3, pp. 1388–1401, March 2014.

[6] A. Elsherif, W.-P. Chen, A. Ito, and Z. Ding, "Resource allocation and inter-cell interference management for dual-access small cells," *IEEE Journal on Selected Areas in Communications*, vol. 33, no. 6, pp. 1082–1096, June 2015.

[7] W. C. Cheung, T. Quek, and M. Kountouris, "Throughput optimization, spectrum allocation, and access control in two-tier femtocell networks," *IEEE Journal on Selected Areas in Communications*, vol. 30, no. 3, pp. 561–574, April 2012.

[8] J. Andrews, S. Singh, Q. Ye, X. Lin, and H. Dhillon, "An overview of load balancing in HetNets: old myths and open problems," *IEEE Wireless Communications*, vol. 21, no. 2, pp. 18–25, April 2014.

[9] T. Wang and L. Vandendorpe, "Iterative resource allocation for maximizing weighted sum min-rate in downlink cellular OFDMA systems," *IEEE Trans. on Signal Processing*, vol. 59, no. 1, pp. 223–234, January 2011.

[10] J. Andrews, H. Claussen, M. Dohler, S. Rangan, and M. Reed, "Femtocells: Past, present, and future," *IEEE Journal on Selected Areas in Communications*, vol. 30, no. 3, pp. 497–508, April 2012.

[11] M. Chen, S. C. Liew, Z. Shao, and C. Kai, "Markov approximation for combinatorial network optimization," *IEEE Trans. on Information Theory*, vol. 59, no. 10, pp. 6301–6327, October 2013.

[12] S. Zhang, Z. Shao, M. Chen, and L. Jiang, "Optimal distributed P2P streaming under node degree bounds," *IEEE/ACM Trans. on Networking*, vol. 22, no. 3, pp. 717–730, June 2014.

[13] J. Jiang, T. Lan, S. Ha, M. Chen, and M. Chiang, "Joint VM placement and routing for data center traffic engineering," in *Proceedings of IEEE INFOCOM*, Orlando, FL, March 2012, pp. 2876–2880.

[14] K. Son, S. Lee, Y. Yi, and S. Chong, "REFIM: A practical interference management in heterogeneous wireless access networks," *IEEE Journal on Selected Areas in Communications*, vol. 29, no. 6, pp. 1260–1272, June 2011.

[15] E. L. Narayanan, *Channel assignment and graph multicoloring*. John Wiley & Sons, 2002.

[16] S. Boyd and L. Vandenberghe, *Convex Optimization*. New York, NY: Cambridge University Press, 2004.

[17] P. Diaconis and D. Stroock, "Geometric bounds for eigenvalues of markov chains," *The Annals of Applied Probability*, vol. 1, no. 1, pp. 36–61, February 1991.

[18] Y. P. D. A. Levin and E. L. Wilmer, *Markov Chains and Mixing Times*. American Mathematical Society, 2009.